Electrical Power and Energy Systems 139 (2022) 107963

Contents lists available at ScienceDirect

International Journal of Electrical Power and Energy Systems

journal homepage: www.elsevier.com/locate/ijepes

Distributed adjustable robust optimal power-gas flow considering wind power uncertainty☆

Junyi Zhai [a,b], Yuning Jiang [c,*], Jianing Li [d], Colin N. Jones [c], Xiao-Ping Zhang [d]

[a] College of New Energy, China University of Petroleum (East China), Qingdao, China
[b] State Grid (suzhou) City & Energy Research Institute, Suzhou, China
[c] Laboratoire d'Automatique, École Polytechnique Fédérale de Lausanne (EPFL), Lausanne, Switzerland
[d] Department of Electronic, Electrical and Systems Engineering, University of Birmingham, Birmingham, United Kingdom

ARTICLE INFO

Keywords:
Integrated electricity and natural gas system (IEGS)
Distributed optimization
Adjustable robust optimization
Linear decision rules (LDRs)
Automatic generation control (AGC)

ABSTRACT

The rapid uptake of natural gas-fired units in energy systems poses significant challenges in coordinating the electricity and gas systems. Besides, the uncertainty caused by integrated renewable energy such as wind power raises more requirements on the robustness of the operation for integrated electricity and natural gas system (IEGS). To address these challenges, this paper investigates the distributed adjustable robust optimal power and gas flow (OPGF) model for IEGS. Using linear decision rules (LDRs), we first propose an improved adjustable robust model combining with the automatic generation control systems to fully exploit its potential in dealing with renewable energy uncertainty while utilizing the controllable polyhedral uncertainty set to reduce solution conservatism. This improved LDRs based adjustable robust approach can reduce the computational burden caused by the existing decomposition based robust approach when applied to distributed optimization. Then, to preserve the information privacy and decision-making independence of subsystems, two tailored alternating direction method of multipliers (ADMM) based distributed optimization frameworks for IEGS with and without a central coordinator are presented, respectively. Effectiveness is illustrated through benchmark case studies.

1. Introduction

Natural gas has already become the second-largest source in the world energy consumption [1]. The advent of low-cost and high-efficiency natural gas has promoted the development of natural gas-fired units (NGUs). Since NGUs serve as producers in electrical networks and consumers in natural gas networks, they closely link these formerly isolated energy systems and optimize them as an integrated electricity and natural gas system (IEGS).

The similarity in gas and electricity consumption profiles gives rise to critical mandates for the coordinated operation of IEGS. A security-constrained planning model for IEGS is presented by [2]. Considering the $N-1$ contingencies, [3] addressed the security-constrained optimal power and gas flow (OPGF) problem. In [4], a robust defense strategy was proposed against malicious attacks for the IEGS. [5] presents a two-stage coordinated operation model for IEGS and electricity–gas-transportation coupled system considering renewable energy uncertainty. In order to construct the model of steady-state gas flow, the quadratic Weymouth equation is widely applied for model simplification. In [6], the convex relaxation of Weymouth equation for joint expansion planning of IEGS is presented. A guaranteed accuracy can be achieved due to the large time constant of gas flow [7], and the second-order cone programming (SOCP) can be employed to represent a tradeoff between fidelity and computational tractability. However, the works mentioned above usually assume a vertically integrated utility that monitors and controls the IEGS. As a result, the individual operator's information diversity and privacy cannot be ensured. In reality, the electricity and natural gas networks may be owned by different utilities [8,9], which can be classified into two architectures according to whether there is a central operator (CO), i.e., the distributed and the decentralized architecture. The electricity operator (EO) and gas operator (GO) are managed by an upper-level CO in the distributed one. Moreover, there is no central coordinator in the decentralized one, and the electricity and natural gas networks are managed by the EO and GO, respectively.

☆ This work was supported in part from the Youth Program of Natural Science Foundation of Jiangsu Province, China (BK20210103) and in part from the Swiss National Science Foundation under the RISK project (Risk Aware Data Driven Demand Response, grant number 200021 175627)

* Corresponding author.
E-mail addresses: zhaijunyi@163.com (J. Zhai), yuning.jiang@epfl.ch (Y. Jiang), J.Li.6@bham.ac.uk (J. Li), colin.jones@epfl.ch (C.N. Jones), X.P.Zhang@bham.ac.uk (X.-P. Zhang).

https://doi.org/10.1016/j.ijepes.2022.107963
Received 16 October 2021; Received in revised form 10 December 2021; Accepted 3 January 2022
Available online 11 February 2022

Various decomposition techniques have been employed to achieve the distributed operation of multi-area power systems, which can be classified into three types: (1) the augmented Lagrangian relaxation based approaches such as the analytical target cascading (ATC) [10–12], alternating direction method of multipliers (ADMM) [13–17] and auxiliary problem principle (APP) [18]; (2) the Karush–Kuhn–Tucker conditions based approaches such as the heterogeneous decomposition (HD) algorithm [19] and the optimality condition decomposition (OCD) algorithm [20]; and (3) the benders decomposition (BD) algorithm [21]. Whereas, the HD, OCD, and BD algorithms are only suitable to solve the deterministic optimization problem [13]. As a classical augmented Lagrangian based algorithm, the alternating direction multiplier method (ADMM) has shown its superiority in convergence property, which has been adopted to the integrated transmission and distribution system scheduling [14], distributed operation of AC/DC hybrid system [16], and distributed power flow [17] problems. However, the research on the distributed operation of IEGS is very limited. Recently, ADMM has been applied to the synergistic operation of IEGS in [22–24]. However, the renewable energy uncertainty is not considered. The decentralized operation for IEGS is recently presented in [25], and the chance-constrained programming is adopted to describe uncertainties; however, the probability distribution information of uncertain variables in these models is hard to obtain.

With the growing integration of wind energy, it is desired to hedge uncertainty for IEGS to achieve a higher overall economic efficiency and reliability. Robust optimization (RO) is a popular method to describe uncertainties. A two-stage RO model formulates the uncertainty in IEGS proposed by [26]. Two-stage RO models consist of the first stage min problem and the second stage max–min problem, which need a decomposition algorithm [27,28] based on the master-subproblem iteration framework to find the robust solution. Unlike the decomposition based robust approach, the linear decision rules (LDRs) model can provide a slightly conservative yet single tractable solution to the adjustable robust formulation. Since the robust counterpart of the LDRs based adjustable approach is usually a tractable convex problem, the LDRs model is more suitable for applying distributed optimization. The linear decision rules have been applied to adjustable robust optimal power flow [29–32], residential distributed generation coordination [33], generation expansion planning [34], and reactive power control [35].

Based on the existing literatures about the LDRs adjustable robust models and distributed optimization models, there are still research gaps that need to be studied.

1. When considering the renewable energy uncertainty in the traditional LDRs-based adjustable robust models, the existing works [29,30] express the uncertainty through allowable output interval, where the AGC participation factors must be predefined such that the resulting model is linear. However, predefining the participation factors is restrictive and thus leads to a conservative solution. Meanwhile, the potential of AGC units cannot be fully exploited to deal with uncertainty. The other previous works [31,32] express the uncertainty through nonadjustable bounded intervals, which are also quite conservative. Moreover, the wind power curtailment situation cannot be handled in these models [29–32]. In short, the relationship between the LDRs model and AGC systems has not been thoroughly studied, especially when the wind power curtailment situation is considered and the uncertainties are expressed through bounded intervals in a controllable polyhedral uncertainty set.
2. Another classical alternate to consider the renewable energy uncertainty is the decomposition-based RO models [26–28]. However, these works mainly have two disadvantages when deploying distributed optimization to deal with the resulting optimization problems. Firstly, the calculation burden will be enlarged as the inner master-subproblem iteration of the decomposition-based algorithm for RO is needed in each outer ADMM iteration. Secondly, the robust counterpart of the second-stage max–min problem in decomposition-based RO models is bilinear and nonconvex. Although this bilinear problem can be either solved by outer approximation method [27] (only local optimality is guaranteed) or rewritten into a MILP problem using the big-M method [26,28], the convergence of ADMM cannot be guaranteed on these nonconvex problems. Therefore, the application of the decomposition-based RO algorithm to distributed optimization faces many limitations.
3. The current distributed operation structures for IEGS has not fully considered the possible infrastructure networks of IEGS, at least not exactly classifies the networks with respect to the existence of the central coordinator. In reality, the IEGS can be classified into two architectures according to whether there exists a central coordinator, so-called the distributed and the decentralized architecture, respectively. Therefore, the applicability of ADMM should be fully exploited for different infrastructure networks specifically based on IEGS.

To fill the research gap in the reported literature, this paper proposes the improved LDRs based distributed adjustable robust OPGF model for IEGS. It is coincident with the AGC systems, and thus, the potential of AGC systems in dealing with wind power uncertainty is fully exploited. Meanwhile, the controllable polyhedral uncertainty set is utilized to control the robustness level of LDRs model. To solve the resulting optimization problem, two tailored ADMM based distributed decision-making strategies are presented. The first strategy considers the network, including a central coordinator, such that the consensus between EO and GO has to be achieved by communicating with the central coordinator. The second one considers a fully decentralized network in which the EO is directly connected with GO, such that only peer-to-peer communication is required to achieve consensus. All costly computations are performed locally in parallel while preserving the information privacy and decision-making independence of subsystems.

1. We propose an improved LDRs based adjustable robust OFGF model. Compared to the prior LDRs based models [29,30] that must predefine the AGC participation factors, our model considers the AGC participation factors as optimization variables to fully exploit the potential of AGC units in dealing with renewable energy uncertainty. Moreover, compared to the other existing LDRs models [31,32], which express uncertain variables through non-adjustable bounded intervals, we present the bounded intervals in a controllable polyhedral uncertainty set. The uncertainty in electricity system transferred to gas system through NGUs is also modeled by LDRs. Furthermore, our improved LDRs model can deal with the wind power curtailment situation, while traditional LDRs models [29–32] are not capable. To the best of our knowledge, this is the first study for the LDRs based adjustable robust model that can simultaneously optimize the AGC participation factors, utilize the budget of uncertainty in a polyhedral uncertainty set, and consider the wind power curtailment situation, leading to significantly less conservative and more practical solutions.
2. Based on two possible topological IEGS, i.e., with and without central coordinator, two tailored ADMM algorithms are proposed to solve the adjustable robust OPGF problem. Both variants solve subproblems individually in parallel with only the NGUs information is shared among subsystems. These improved LDRs based adjustable robust extension of ADMM methods are capable of handling uncertainties in IEGS. To avoid the computational burden caused by too many master-subproblem iterations of the decomposition based robust approach [27,28] when applied to distributed optimization, LDRs are utilized to recast the adjustable robust OPGF problem into a single tractable convex problem including both adjustable and non-adjustable terms. This LDRs model can reduce the computation burden of

each ADMM iteration and guarantee the convergence of ADMM, which eliminates the need for using any master-subproblem decomposition strategy and can be easily applied to distributed optimization.

This paper is organized as follows: Section 2 presents the OPGF formulation. Section 3 addresses the LDRs based adjustable robust OPGF model. Section 4 proposes two tailored ADMM based distributed frameworks. Section 5 presents case studies. Section 6 concludes this paper.

2. Problem formulation of OPGF model for IEGS

This section presents an OPGF model for IEGS. In particular, we consider a wind-integrated power system denoted by the tuple $(\mathcal{B}, \mathcal{L}, \mathcal{NG}, \mathcal{G}, \mathcal{W})$ for electricity network and the tuple $(\mathcal{N}, \mathcal{GP}, \mathcal{GW}, \mathcal{GS}, \mathcal{GC})$ for gas system. Here, $\mathcal{B}$ is the set of buses, $\mathcal{L} \subseteq \mathcal{B} \times \mathcal{B}$ the set of transmission lines, $\mathcal{NG} \subseteq \mathcal{B}$ the set of NGUs, $\mathcal{G} \subseteq \mathcal{B}$ the set of NGUs and non-NGUs, and $\mathcal{W} \subseteq \mathcal{B}$ the set of wind farms. Similarly, $\mathcal{N}$ denotes the set of nodes in gas system, $\mathcal{GP} \subseteq \mathcal{N} \times \mathcal{N}$ the set of pipelines, $\mathcal{GW} \subseteq \mathcal{N}$ the set of gas wells, $\mathcal{GS} \subseteq \mathcal{N}$ the set of gas storages, and $\mathcal{GC} \subseteq \mathcal{N}$ the set of compressors.

2.1. Objective of coordination

The objective of the OPGF problem is to minimize the total operation cost of the electricity network and natural gas network. Natural gas suppliers are gas well and gas storage facilities that provide the natural gas through its transmission network. Natural gas supplies are modeled as positive gas injections at related nodes. The objective in the OPGF problem is then divided into two parts, the fuel cost of non-NGUs given by

$$M_1 = \sum_{i \in \mathcal{G} \setminus \mathcal{NG}} \left\{ c_{1i} \left(\hat{P}_i^G \right)^2 + c_{2i} \hat{P}_i^G + c_{3i} \right\}, \tag{1}$$

and the gas production cost of gas wells and storages given by

$$M_2 = \sum_{m \in \mathcal{GW}} \left(p_m^W F_m^W \right) + \sum_{n \in \mathcal{GS}} \left(p_n^S F_n^S \right). \tag{2}$$

Here, c_{1i}, c_{2i}, and c_{3i} denote the cost coefficients of unit i, $\hat{P}_i^G$ (MW) denotes the reference base-point output of unit i in the nominal scenario, p_m^W (\$/kcf) and p_n^S (\$/kcf) denote the gas production cost of gas well at node m and storage at node n, F_m^W (kcf) and F_n^S (kcf) denote the gas well output at node m and storage output at node n.

2.2. Separative constraints of natural gas system

The typical static characteristics of gas system are given by

$$F_m^W + F_m^S - F_m^G - F_m^D - \sum_{k \in \Psi_m^C} \mu_k^C = \sum_{n \in \Psi_m} F_{mn} + \sum_{k \in \Psi_m^C} F_k^C \ , \ m \in \mathcal{N} \tag{3a}$$

$$F_{mn} = C_{mn} \sqrt{\pi_m^2 - \pi_n^2} \ , \ (m,n) \in \mathcal{GP} \tag{3b}$$

$$\pi_n \le \pi_m \ , \ (m,n) \in \mathcal{GP} \tag{3c}$$

$$\underline{\pi}_m \le \pi_m \le \overline{\pi}_m \ , \ m \in \mathcal{N} \tag{3d}$$

$$\underline{F}_m^W \le F_m^W \le \overline{F}_m^W \ , \ m \in \mathcal{N} \tag{3e}$$

$$\underline{F}_m^S \le F_m^S \le \overline{F}_m^S \ , \ m \in \mathcal{N} \tag{3f}$$

$$0 \le F_{mn} \le \overline{F}_{mn} \ , \ (m,n) \in \mathcal{GP} \tag{3g}$$

$$0 \le F_k^C \le \overline{F}_k^C \ , \ k \in \mathcal{GC} \tag{3h}$$

$$\mu_k^C = \gamma_k F_k^C \ , \ k \in \mathcal{GC} \tag{3i}$$

$$\underline{r}_k \le \pi_k^{out} / \pi_k^{in} \le \overline{r}_k \ , \ k \in \mathcal{GC} \tag{3j}$$

where Ψ_m and Ψ_m^C denote the gas nodes and gas compressors connected to node m, respectively, F_m^G (kcf) the gas consumption of NGU at node m, F_{mn} (kcf) the gas flow through pipeline $(m,n) \in \mathcal{GP}$, F_k^C (kcf) the gas flow through gas compressor k, F_m^D (kcf) the gas demands at node m, $\overline{F}_{mn}$ (kcf) the maximum allowable gas flow of pipeline $(m,n) \in \mathcal{GP}$, C_{mn} (kcf/Psig) the Weymouth constant of pipeline $(m,n) \in \mathcal{GP}$, π_m (Psig) the gas pressure of node m, $\underline{\pi}_m$ (Psig) and $\overline{\pi}_m$ (Psig) denote the maximum and minimum gas pressure of node m, respectively, π_k^{out} (Psig) and π_k^{in} (Psig) denote the outlet and inlet pressures of gas compressor k, respectively, μ_k^C (kcf) the gas consumption caused by gas compressor k, γ_k the energy conversion efficiency of gas compressor k, $\underline{r}_k$ and $\overline{r}_k$ denote the maximum and minimum compression ratio of gas compressor k, respectively.

Eq. (3a) describes the nodal gas flow balance. Eq. (3b) describes the steady-state Weymouth gas flow model [7]. Since the gas flow directions are always pre-specified according to the gas-transmission-system operation practice in intra-day stage [36], the bi-directional gas flow is not considered here. This setting is similar to the distributed dispatch model for IEGS proposed in [37], which is a reasonable assumption in the short-term OPGF problem, whereas the long-term operation or planning decision should consider bi-directional gas flows [38]. (3c) and (3d) denote the nodal pressure. Gas well and storage supply constraints are given in (3e) and (3f), respectively. (3g) and (3h) denote the limit of gas pipelines and compressors, respectively. The gas consumptions of compressors represent a specified percentage of the transported gas flow as given in (3i), while (3j) denotes the compression ratio limit of outlet and inlet gas pressures.

2.3. Separative constraints of electricity system

The typical constraints of electricity system are given by

$$\begin{cases} \hat{P}_i^G = 0 \ , \ i \in \mathcal{B} \setminus \mathcal{G} \ , \ \ \hat{P}_i^W = 0 \ , \ i \in \mathcal{B} \setminus \mathcal{W} \\ \hat{P}_i^G + \hat{P}_i^W - \sum_{j \in \mathcal{B}_i} \dfrac{\hat{\theta}_i - \hat{\theta}_j}{x_{ij}} = P_i^D, \ i \in \mathcal{B} \end{cases} \tag{4a}$$

$$0 \le P_i^W \le \overline{P}_i^W \ , \ i \in \mathcal{W} \tag{4b}$$

$$\underline{P}_i^G \le P_i^G \le \overline{P}_i^G \ , \ i \in \mathcal{G} \tag{4c}$$

$$-\overline{L}_{ij} \le \frac{\theta_i - \theta_j}{x_{ij}} \le \overline{L}_{ij} \ , \ (i,j) \in \mathcal{L} \tag{4d}$$

$$\theta_1^{\text{ref}} = 0 \tag{4e}$$

where $\mathcal{B}_i$ denotes the neighboring buses of bus i, $\hat{P}_j^W$ (MW) denotes the reference base-point output of wind farm j in the nominal scenario, $\hat{\theta}_i$ (rad) denotes the reference base-point of phase angle of bus i in the nominal scenario, P_i^G (MW) and P_i^W (MW) respectively denote the output from unit i and wind farm i under the realization of wind generation, θ_i (rad) denotes the phase angle of bus i under the realization of wind generation, P_i^D (MW) denotes the load demand at bus i, x_{ij} (p.u.) and $\overline{L}_{ij}$ (MW) denote the reactance and capacity of transmission line $(i,j) \in \mathcal{L}$, respectively, $\underline{P}_i^G$ (MW) and $\overline{P}_i^G$ (MW) denote the minimum and maximum output for all $i \in \mathcal{G}$, respectively, $\overline{P}_i^W$ (MW) denotes the wind farm forecasts for all $i \in \mathcal{W}$.

Constraint (4a) describes the nodal power balance in the nominal scenario. (4b) denotes the wind farm output limit. (4c) denotes the unit output limit, including the NGUs and non-NGUs (4d) denotes the power flow limit of the transmission line. (4e) defines bus 1 as the reference bus in the system. Here, the commonly used approximate linear DC power flow model is adopted for the transmission level IEGS [22,25,39–41].

2.4. Coupling between electricity and natural gas system

NGUs represent the linkages between gas and electricity networks, which can also be utilized to deal with renewable energy uncertainty.

The relationship between generation output and gas consumption of NGUs can be described as

$$F_m^G = \omega_i P_i^G,\ (m,i) \in \Omega \tag{5}$$

where Ω denotes the pairs of node $m \in \mathcal{N}$ and its equipped NGU $i \in \mathcal{NG}$, ω_i denotes the conversion coefficient of NGU i.

The gas consumption of the ith NGU in the electricity network is fed by gas extracted from the mth gas node in the gas network. Eq. (5) assumes a linear relationship [9,42] between the gas consumption of NGUs and their power outputs under the realization of wind power generation, which ensures the safe operation of the gas system under wind power uncertainty.

2.5. Second-order cone reformulation for natural gas system

The nonconvex relationship between pipeline gas flow and the nodal squared pressure drop is denoted by (3b), which makes the optimal gas flow problem in gas network nonconvex. SOC relaxation is an effective way for convexification. However, convexification should be exact for the feasible region to stay the same compared to the original primal problem. Here, we apply SOC relaxation introduced in [7] to deal with the nonconvexity of (3b). In a result, we have convex second-order cone constraints derived by

$$\begin{aligned} &F_{mn} = C_{mn}\sqrt{\pi_m^2 - \pi_n^2} \rightarrow F_{mn}^2/C_{mn}^2 = \pi_m^2 - \pi_n^2 \\ &\rightarrow F_{mn}^2/C_{mn}^2 + \pi_n^2 \le \pi_m^2 \rightarrow \left\| \begin{bmatrix} F_{mn}/C_{mn} \\ \pi_m \end{bmatrix} \right\|_2 \le \pi_m\,. \end{aligned} \tag{6}$$

If the solution satisfies (3b), the relaxation is exact and the solution is globally optimal. However, the relaxation (6) may not always be tight during the iteration of optimization algorithm. To drive the exactness of SOC relaxation, an additional penalty term

$$M_3 = \sum_{(m,n)\in\mathcal{GP}} \beta\left(\pi_m - \pi_n\right)$$

with positive constant β is added to the objective function, which drives the $\pi_m^2 - \pi_n^2$ toward F_{mn}^2/C_{mn}^2 [22]. This positive linear penalty term makes the violation of the constraint (3b) smaller.

3. LDRs based adjustable Robust OPGF model for IEGS

This section presents an LDRs based adjustable robust OPGF model for IEGS coincident with the AGC systems. The AGC participation factors are treated as optimizable variables and then the LDRs and AGC systems are fully combined to utilize the capability of AGC units to deal with wind power uncertainty in a controllable polyhedral uncertainty set.

3.1. Uncertainty characterization

The fluctuations in renewable energy generation represent the major degree of uncertainty and these uncertainties will be propagated from the electricity system to the gas system via NGUs, which offers a considerable operational challenge to gas networks. The randomness of wind farm output is described through bounded intervals in a controllable polyhedral uncertainty set to reduce solution conservatism as follows:

$$\mathcal{U} = \left\{ P^W \in \mathbb{R}^{|\mathcal{W}|} \;\middle|\; \begin{Bmatrix} \forall k \in \mathcal{W},\ |z_k| \le 1 \\ \tilde{P}_k^W = \overline{P}_k^W + \Delta P_k^W z_k, \end{Bmatrix} \right\}. \tag{7}$$

Here, $\tilde{P}_k^W$ denotes the uncertain wind farm output, and ΔP_k^W denotes the deterministic maximum magnitude of the deviation from forecasts. Moreover, we introduce the auxiliary variable z_k to denote the upward/downward deviation from forecasts. The choice of σ aims at adjusting the solution conservativeness. Specifically, choosing $\sigma = 0$ leads to the deterministic model, since uncertain parameters cannot deviate from their forecasts. However, choosing $\sigma > 0$ leads to the robust model where the uncertain parameters can deviate from their forecasts.

3.2. Adjustable robust OPGF model

To derive a tractable form for the adjustable robust OPGF model, the following LDRs are considered,

$$P_j^W = \hat{P}_j^W - \sum_{k\in\mathcal{W}} \beta_{jk}\left(\tilde{P}_k^W - \overline{P}_k^W\right),\ j \in \mathcal{W}, \tag{8a}$$

$$P_g^G = \hat{P}_g^G - \alpha_g \sum_{k\in\mathcal{W}} \left(\tilde{P}_k^W - \overline{P}_k^W\right),\ g \in \mathcal{G}, \tag{8b}$$

$$1 = \sum_{g\in\mathcal{G}} \alpha_g \quad \text{with}\ \ \alpha_g \in [0,1],\ g \in \mathcal{G}, \tag{8c}$$

where $\hat{P}_g^G$ and $\hat{P}_j^W$ are the non-adjustable terms in the nominal scenario. α_g and β_{jk} respectively denote the adjustable terms for units g and wind farm j under the realization of wind generation, and α_g is directly compatible with the AGC participation factors.

The LDRs based adjustable robust OPGF model can be obtained from (4) and (5) by replacing the certain wind farm forecasts $\overline{P}_i^W$ with their uncertain values $\tilde{P}_i^W$ and using the above-mentioned LDRs. Let us first have a look at the right hand side of (4c). Substituting (8) into the right hand side of (4c) yields the worst possible inequality

$$\overline{P}_g^G - \hat{P}_g^G \ge -\alpha_g \cdot \max_{P^W\in\mathcal{U}} \sum_{k\in\mathcal{W}} \left(P_k^W - \hat{P}_k^W\right),\ g \in \mathcal{G}\,. \tag{9}$$

The inner maximization problem in (9) is equivalent to

$$\max_{z\in\mathbb{R}^{2|\mathcal{W}|}} \quad \sum_{k\in\mathcal{W}} \Delta P_k^W \left(z_k^+ - z_k^-\right) \tag{10a}$$

$$\text{s.t.} \quad 0 \le z_k^+ \le 1, \quad k \in \mathcal{W} \quad | \ \kappa_k^{*+} \tag{10b}$$

$$0 \le z_k^- \le 1, \quad k \in \mathcal{W} \quad | \ \kappa_k^{*-} \tag{10c}$$

$$z_k^+ + z_k^- \le 1, \quad k \in \mathcal{W} \quad | \ \kappa_k^{*1} \tag{10d}$$

$$\sum_{k\in\mathcal{W}} \left(z_k^+ + z_k^-\right) \le \sigma, \quad | \ \mu^* \tag{10e}$$

where κ_k^{*+}, κ_k^{*-}, κ_k^{*1}, and μ^* represent the dual variables with respect to the polyhedral constraints. In the following, the wild-char superscript * is substituted by $G(r)$, $G(l)$, $W(r)$, $W(l)$, $L(r)$, $L(l)$, and N in (11), (38), (12), (39), (13), (40), and (16), respectively. These superscripts are characters only used to discriminate the dual variables. Using the duality of (10) leads to the LDRs based robust formulation:

$$\overline{P}_g^G - \hat{P}_g^G \ge \sum_{k\in\mathcal{W}} \left(\kappa_{gk}^{G(r)+} + \kappa_{gk}^{G(r)-} + \kappa_{gk}^{G(r)1}\right) + \sigma\mu_g^{G(r)}, \tag{11a}$$

$$-\alpha_g \Delta P_k^W \le \kappa_{gk}^{G(r)+} + \kappa_{gk}^{G(r)1} + \mu_g^{G(r)}, \tag{11b}$$

$$\alpha_g \Delta P_k^W \le \kappa_{gk}^{G(r)-} + \kappa_{gk}^{G(r)1} + \mu_g^{G(r)}, \tag{11c}$$

$$\kappa_{gk}^{G(r)+} \ge 0,\ \kappa_{gk}^{G(r)-} \ge 0,\ \kappa_{gk}^{G(r)1} \ge 0,\ \mu_g^{G(r)} \ge 0 \tag{11d}$$

for all $k \in \mathcal{W}$ and $g \in \mathcal{G}$. In a result, constraint (9) can be replaced by affine equality constraints (11).

Similarly, the LDRs based adjustable robust form for the right hand side of (4b) can be derived as

$$\overline{P}_j^W - \hat{P}_j^W \ge \sum_{k\in\mathcal{W}} (\kappa_{jk}^{W(r)+} + \kappa_{jk}^{W(r)-} + \kappa_{jk}^{W(r)1}) + \sigma\mu_j^{W(r)}, \quad j \in \mathcal{W} \tag{12a}$$

$$-\left(\beta_{jk}+1\right)\Delta P_k^W \le \kappa_{jk}^{W(r)+} + \kappa_{jk}^{W(r)1} + \mu_j^{W(r)},\ j = k \tag{12b}$$

$$\left(\beta_{jk}+1\right)\Delta P_k^W \le \kappa_{jk}^{W(r)-} + \kappa_{jk}^{W(r)1} + \mu_j^{W(r)},\ j = k \tag{12c}$$

$$-\beta_{jk}\Delta P_k^W \le \kappa_{jk}^{W(r)+} + \kappa_{jk}^{W(r)1} + \mu_j^{W(r)},\ j \in \mathcal{W}, j \ne k \tag{12d}$$

$$\beta_{jk}\Delta P_k^W \le \kappa_{jk}^{W(r)-} + \kappa_{jk}^{W(r)1} + \mu_j^{W(r)},\ j \in \mathcal{W}, j \ne k \tag{12e}$$

$$\kappa_{jk}^{W(r)+} \geq 0\,,\ \kappa_{jk}^{W(r)-} \geq 0\,,\ \kappa_{jk}^{W(r)1} \geq 0\,,\ \mu_{j}^{W(r)} \geq 0 \tag{12f}$$

for all $k \in \mathcal{W}$.

Note that the voltage angles in (4d) can be divided into two components as well, the non-adjustable component associated with predictive quantities and the adjustable component that varies with the uncertain wind forecast error, as shown in Appendix-A. With the uncertainty directly included in branch flow, the uncertain power flow in branch can also be written as a equivalent set of linear constraints. Regarding the right hand side of (4d), the LDRs based form is given by

$$\overline{L}_{ij} + \frac{\hat{\theta}_i - \hat{\theta}_j}{x_{ij}} \geq \sum_{k\in\mathcal{W}} \left(\kappa_{ijk}^{L(r)+} + \kappa_{ijk}^{L(r)-} + \kappa_{ijk}^{L(r)1}\right) + \sigma\mu_{ij}^{L(r)}, \tag{13a}$$

$$\frac{1}{x_{ij}}\left(\tilde{B}_{jk}\beta_{jk} - \tilde{B}_{ik}\beta_{ik} + \sum_{g\in\mathcal{G}}\tilde{B}_{jg}\alpha_i - \sum_{g\in\mathcal{G}}\tilde{B}_{ig}\alpha_i\right)$$

$$\Delta P_k^W \ \leq\ \kappa_{ijk}^{L(r)+} + \kappa_{ijk}^{L(r)1} + \mu_{ij}^{L(r)}, \tag{13b}$$

$$-\ \frac{1}{x_{ij}}\left(\tilde{B}_{jk}\beta_{jk} - \tilde{B}_{ik}\beta_{ik} + \sum_{i\in\mathcal{G}}\tilde{B}_{jg}\alpha_i - \sum_{g\in\mathcal{G}}\tilde{B}_{ig}\alpha_i\right)$$

$$\Delta P_k^W \ \leq\ \kappa_{ijk}^{L(r)-} + \kappa_{ijk}^{L(r)1} + \mu_{ij}^{L(r)}, \tag{13c}$$

$$\kappa_{ijk}^{L(r)+} \geq 0,\ \kappa_{ijk}^{L(r)-} \geq 0,\ \kappa_{ijk}^{L(r)1} \geq 0,\ \mu_{ij}^{L(r)} \geq 0 \tag{13d}$$

for all $k \in \mathcal{W}$ and $(i,j) \in \mathcal{L}$. $\tilde{B}_{ik}$ and $\tilde{B}_{jk}$ denote the element of electricity network admittance inverse matrix, with the reference angle at bus 1. The same approach can be applied to the left hand side of (4b), (4c), and (4d), shown in Appendix-B.

The electricity and natural gas coupling constraint (5) can also be directly converted into the following form, which is always tight since the unnecessary natural gas consumption by NGUs will lead to higher operation costs.

$$F_m^G \geq \omega_i P_i^G,\ (m,i) \in \Omega. \tag{14}$$

Substituting (8) into (14) yields the worst possible inequality

$$F_m^G - \omega_i \hat{P}_i^G \geq -\omega_i\alpha_i \cdot \max_{\boldsymbol{P}^W\in\mathcal{U}} \sum_{k\in\mathcal{W}} \left(P_k^W - \hat{P}_k^W\right),\ (m,i) \in \Omega. \tag{15}$$

Using the duality of (10), the LDRs based adjustable robust form of (5) can be derived as

$$F_m^G - \omega_i \hat{P}_i^G \geq \sum_{k\in\mathcal{W}} \left(\kappa_{ik}^{N+} + \kappa_{ik}^{N-} + \kappa_{ik}^{N1}\right) + \sigma\mu_i^N, \tag{16a}$$

$$-\omega_i\alpha_i\Delta P_k^W \ \leq \kappa_{ik}^{N+} + \kappa_{ik}^{N1} + \mu_i^N, \tag{16b}$$

$$\omega_i\alpha_i\Delta P_k^W \ \leq \kappa_{ik}^{N-} + \kappa_{ik}^{N1} + \mu_i^N, \tag{16c}$$

$$\kappa_{ik}^{N+} \geq 0\,,\ \kappa_{ik}^{N-} \geq 0\,,\ \kappa_{ik}^{N1} \geq 0\,,\ \mu_i^N \geq 0 \tag{16d}$$

for all $(m,i) \in \Omega$ and $k \in \mathcal{W}$.

Finally, we obtain the LDRs based adjustable robust OPGF model for IEGS as follows:

$$\begin{aligned} &\text{minimize} \quad M_1 + M_2 + M_3 \\ &\text{subject to} \quad (3),\ (4a),\ (4e),\ (11)\text{–}(13),\ (16),\ (38)\text{–}(40). \end{aligned} \tag{17}$$

This problem aims at minimizing the base-case operation cost in nominal scenario, while adaptively and securely adjusting the output of AGC units in response to possible realizations of wind power uncertainties. This adjustable robust OPGF model does not need any decomposition-based robust algorithm and can be directly solved by commercial solvers.

Overall, the proposed model (17) is a convex quadratic programming with convex SOC constraints. It can only be directly solved in a centralized manner. In reality, the operation for the electricity system and gas system is owned by different utilities. Only limited information on NGUs can be shared between electricity system and gas system to ensure consistency in operating, which is an independent decision-making process. Therefore, the entire problem is preferable to be solved in a distributed way to preserve the information privacy and the independent decision of different operators.

4. Distributed optimization for adjustable robust OPGF

In this section, we tailor the ADMM algorithm [14,43] to solve the OPGF problem. Moreover, we address how to implement the algorithm under two network configurations based IEGS, one is with a central coordinator and one is not, which represent two different styles to operate the IEGS.

4.1. ADMM for OPGF

The key of applying ADMM to solve the OPGF problem in a distributed manner is to achieve consensus between the EO and GO with respect to the coupling constraint (5). However, ADMM is only capable of dealing with linear couplings. To this end, we introduce consensus variables r_{mi} and the affine equality constraints

$$\begin{cases} F_m^G - r_{mi} = 0 & | \ \lambda_{mi}^G \\ F_i^E - r_{mi} = 0 & | \ \lambda_{mi}^E \end{cases} \tag{18}$$

for all $(m,i) \in \Omega$. Here, F_i^E denotes the duplicated gas consumption of NGU at bus i in electricity network such that F_m^G and F_i^E are bundled by the additional consensus variable r_{mi}, λ_{mi}^G and λ_{mi}^E define the corresponding Lagrangian multipliers. In a result, the constraint (14) becomes fully local with respect to the electricity system as follows:

$$F_i^E \geq \omega_i P_i^G\,. \tag{19}$$

As the main idea of ADMM is to dualize the consensus constraint (18) using augmented Lagrangian, in order to construct a universal framework for two different network configurations, we define the quadratic terms by functions $\boldsymbol{\Phi}_{mi}^E : \mathbb{R}\times\mathbb{R} \to \mathbb{R}_{\geq 0}$ and $\boldsymbol{\Phi}_{mi}^G : \mathbb{R}\times\mathbb{R} \to \mathbb{R}_{\geq 0}$,

$$\boldsymbol{\Phi}_{mi}^E(F_i^E, \tilde{F}_i^E) = (F_i^E - \tilde{F}_i^E)^2\,,\ \boldsymbol{\Phi}_{mi}^G(F_i^G, \tilde{F}_i^G) = (F_i^G - \tilde{F}_i^G)^2$$

for all $(m,i) \in \Omega$, where inputs $\tilde{F}_i^E$ and $\tilde{F}_i^G$ can be considered as reference of F_i^E and F_i^G varying in iterations. Accordingly, we summarize the standard ADMM for solving the OPGF problem as the following two steps, a parallelizable step and a consensus step. Here, notation τ indicates the τ-th iteration.

1. *Parallelizable Step:* Solve the following two problems in parallel by EO and GO, respectively.

   (a) Subproblem $\mathscr{P}_E$:

   $$\begin{aligned} &\min\ M_1 + \frac{\rho}{2}\sum_{(m,i)\in\Omega} \boldsymbol{\Phi}_{mi}^E\left(F_i^E, r_{mi}(\tau) - \frac{\lambda_{mi}^E(\tau)}{\rho}\right) \\ &\text{subject to (4a), (4e), (11)–(13), (16), (38)–(40).} \end{aligned} \tag{20}$$

   (b) Subproblem $\mathscr{P}_G$:

   $$\begin{aligned} &\min\ M_2 + M_3 + \frac{\rho}{2}\sum_{(m,i)\in\Omega} \boldsymbol{\Phi}_{mi}^G\left(F_m^G, r_{mi}(\tau) - \frac{\lambda_{mi}^G(\tau)}{\rho}\right) \\ &\text{subject to (3).} \end{aligned} \tag{21}$$

   Noted that in subproblem $\mathscr{P}_E$, variable F_m^G in constraints (16) has been replaced by F_i^E according to (19) such that it is only with respect to the $\mathscr{P}_E$. Based on the proposed LDRs based robust model in Section 3, subproblems $\mathscr{P}_E$ and $\mathscr{P}_G$ are formulated by using the augmented Lagrangian to construct the models $\boldsymbol{\Phi}_{mi}^E$ and $\boldsymbol{\Phi}_{mi}^G$ [14] with positive weighting $\rho > 0$. Here, as the SOC relaxation is applied to the steady-state Weymouth gas flow model, (21) is a convex SOCP.

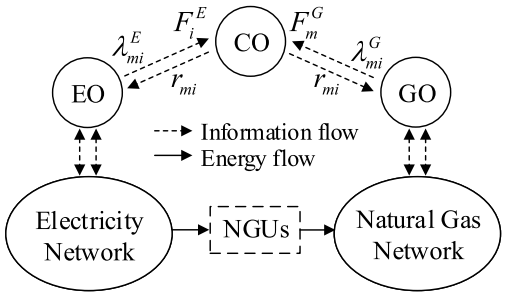

Fig. 1. Architecture with a central coordinator.

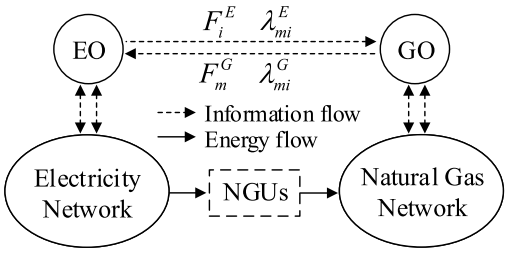

Fig. 2. Architecture without a central coordinator.

2. *Consensus Step:* The upper-level central coordinator is only responsible for handling the coupling constraints between the two networks. In order to update the primal consensus, the upper-level CO computes

$$\begin{aligned} r_{mi}(\tau+1) = \arg\min_{r_{mi}} \ & \Phi_{mi}^E\left(F_i^E(\tau+1), r_{mi} - \frac{\lambda_{mi}^E(\tau)}{\rho}\right) \\ & + \Phi_{mi}^G\left(F_m^G(\tau+1), r_{mi} - \frac{\lambda_{mi}^G(\tau)}{\rho}\right) \\ = & \frac{F_i^E(\tau+1) + F_m^G(\tau+1)}{2} + \frac{\lambda_{mi}^E(\tau) + \lambda_{mi}^G(\tau)}{2\rho} \end{aligned} \tag{22}$$

for all $(m,i) \in \Omega$. Here, $F_i^E(\tau+1)$ and $F_i^G(\tau+1)$ is given by the solution of (20) and (21), respectively. Then, the dual consensus is updated by b

$$\lambda_{mi}^E(\tau+1) = \lambda_{mi}^E(\tau) + \rho\left[F_i^E(\tau+1) - r_{mi}(\tau+1)\right], \tag{23a}$$

$$\lambda_{mi}^G(\tau+1) = \lambda_{mi}^G(\tau) + \rho\left[F_m^G(\tau+1) - r_{mi}(\tau+1)\right]. \tag{23b}$$

As the OPGF problem is convex but not strongly convex, the sublinear convergence rate $\mathcal{O}(1/\tau)$ established in [44] can be directly applied to the standard ADMM above.

4.2. Configuration with central coordinator

When the electricity network is coupled with the natural gas system via a central coordinator, the entire system becomes a distributed architecture. The EO and GO can be considered as two lower-level agents while the upper-level CO coordinates the lower-level agents. The communication strategy is illustrated in Fig. 1. The ADMM for solving the OPGF problem can be summarized as follows into two main steps, a parallelizable step and a consensus step. Algorithm 1 outlines the tailored ADMM for the configuration with a CO.

Compared to the standard framework, the dual updates (23a) and (23b) are executed in parallel in EO and GO. After that, the lower-level subproblems (20) and (21) are solved locally via EO and GO in parallel. Therefore, each lower-level decision-maker can operate their individual systems independently with considering that only the NGUs' information is shared with the central coordinator.

Algorithm 1 ADMM Variant I: distributed consensus

Initialization:

- EO chooses initial guess $F_i^E(0)$ and $\lambda_{mi}^E(0)$ for all $(m,i) \in \Omega$;
- GO chooses initial guess $F_i^G(0)$ and $\lambda_{mi}^G(0)$ for all $(m,i) \in \Omega$;
- CO chooses initial guess $r_{mi}(0)$ for all $(m,i) \in \Omega$.

Repeat:

1. *Parallelizable Step:*

   a) EO receives $r_{mi}(\tau)$ and update

   $$\lambda_{mi}^E(\tau+1) = \lambda_{mi}^E(\tau) + \rho\left[F_i^E(\tau) - r_{mi}(\tau)\right] \tag{24}$$

   Then, solve $\mathscr{P}_E$ with $\Phi_{mi}^E\left(F_i^E, r_{mi}(\tau) - \frac{\lambda_{mi}^E(\tau+1)}{\rho}\right)$ and send solutions $(F_i^E(\tau+1), \lambda_{mi}^E(\tau+1))$ to CO.

   b) GO receives $r_{mi}(\tau)$ and update

   $$\lambda_{mi}^G(\tau+1) = \lambda_{mi}^G(\tau) + \rho\left[F_m^G(\tau) - r_{mi}(\tau)\right] \tag{25}$$

   Then, solve $\mathscr{P}_G$ with $\Phi_{mi}^G\left(F_m^G, r_{mi}(\tau) - \frac{\lambda_{mi}^G(\tau+1)}{\rho}\right)$ and send solutions $(F_i^G(\tau+1), \lambda_{mi}^G(\tau+1))$ to CO.

2. *Consensus Step:* CO collects from EO and GO

   $(F_i^E(\tau+1), \lambda_i^E(\tau+1))$ and $(F_i^G(\tau+1), \lambda_i^G(\tau+1))$

   and then, update the primal consensus by

   $$r_{mi}(\tau+1) = \frac{F_i^E(\tau+1) + F_m^G(\tau+1)}{2} + \frac{\lambda_{mi}^E(\tau+1) + \lambda_{mi}^G(\tau+1)}{2\rho} \tag{26}$$

   and spread it to EO and GO.

4.3. Configuration without central coordinator

When the electricity network is directly connected with the natural gas system, each decision-makers need autonomously and simultaneously to operate their local systems with the consideration that only limited information on NGUs is exchanged. Fig. 2 shows this decentralized structure, where the GO and EO can only establish a peer-to-peer communication channel to achieve cooperation between the two infrastructures. Accordingly, Algorithm 2 outlines the second variant of ADMM with fully decentralized consensus.

The main idea of decentralized consensus is to avoid directly computing the primal consensus r_{mi} at each iterations. To this end, we substitute the explicit form (26) into the dual consensus update (24) and (25) yielding the dual update (27) and (28). Then, the quadratic model $\Phi_{mi}^E\left(F_i^E, \frac{\lambda_{mi}^G(\tau)}{\rho} + F_m^G(\tau)\right)$ and $\Phi_{mi}^G\left(F_m^G, \frac{\lambda_{mi}^E(\tau)}{\rho} + F_i^E(\tau)\right)$ are constructed by substituting (27) and (28) into (20) and (21).

5. Numerical results

A 6-bus-6-node and a 118-bus-20-node IEGS are used and implemented on `Matlab R2016a` with an Intel Core i5-6500, 3.2 GHz, 16 GB RAM computer, using `Gurobi 9.0`. The network parameters

Algorithm 2 ADMM Variant II: decentralized consensus

Initialization:

- EO chooses initial guess $F_i^E(0)$ and $\lambda_{mi}^E(0)$ for all $(m,i) \in \Omega$;
- GO chooses initial guess $F_i^G(0)$ and $\lambda_{mi}^G(0)$ for all $(m,i) \in \Omega$.

Repeat two parallel steps:

a) EO receives $(F_m^G(\tau), \lambda_{mi}^G(\tau))$ and update

$$\lambda_{mi}^E(\tau+1) = \frac{\lambda_{mi}^E(\tau) - \lambda_{mi}^G(\tau)}{2} + \rho \frac{F_i^E(\tau) - F_m^G(\tau)}{2} \tag{27}$$

Then, solve $\mathscr{P}_E$ with $\Phi_{mi}^E\left(F_i^E, \frac{\lambda_{mi}^G(\tau)}{\rho} + F_m^G(\tau)\right)$ and send solutions $(F_i^E(\tau+1), \lambda_{mi}^E(\tau+1))$ to GO.

b) GO receives $(F_i^E(\tau), \lambda_{mi}^E(\tau))$ and update

$$\lambda_{mi}^G(\tau+1) = \frac{\lambda_{mi}^G(\tau) - \lambda_{mi}^E(\tau)}{2} + \rho \frac{F_m^G(\tau) - F_i^E(\tau)}{2} \tag{28}$$

Then, solve $\mathscr{P}_G$ with $\Phi_{mi}^G\left(F_m^G, \frac{\lambda_{mi}^E(\tau)}{\rho} + F_i^E(\tau)\right)$ and send solutions $(F_m^G(\tau+1), \lambda_{mi}^G(\tau+1))$ to EO.

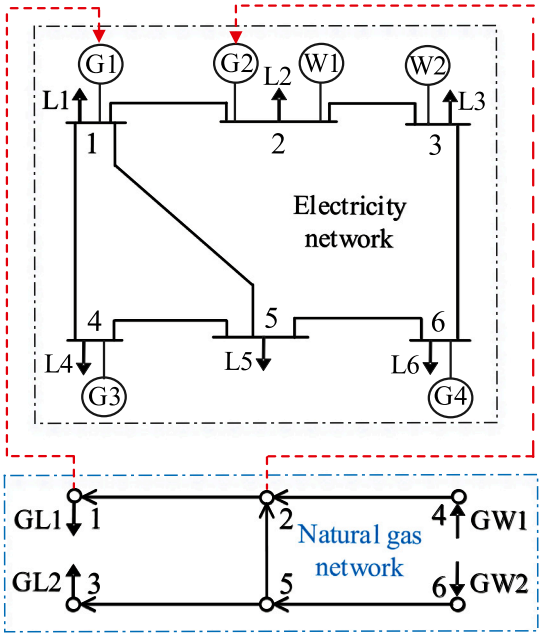

Fig. 3. 6-bus-6-node IEGS.

and other data are available online [45]. Note that the only difference between Algorithms 1 and 2 is the communication strategy. Thus, the solutions from Algorithm 1 are adopted to evaluate the solution accuracy.

5.1. 6-Bus-6-Node IEGS

Case 1 is a 6-bus-6-node IEGS with fixed natural gas flow directions as shown in Fig. 3. The system has 2 NGUs, 2 non-NGUs, 2 wind farms, 7 branches, 6 electricity loads, 2 natural gas wells, 5 pipelines, and 2 gas loads. Variations of wind generation are considered as 20% of their forecast values. In the ADMM procedure, the penalty factor ρ is set as 0.002. Convergence tolerance of the primal and dual residues is 0.01 kcf. The initial values of gas consumptions of NGUs and multipliers are all set at zero.

Table 1
Comparisons with varying budgets for Case 1.

Scheme	Budget	Ite.	Gas (kcf)		Operation cost ($)		
			NGU 1	NGU 2	EO	GO	Total
Cen.	0	–	1876	426	5220	8704	13 924
	1	–	1960	1036	4576	9744	14 320
	2	–	1844	1780	4041	10 687	14 728
Dis.	0	33	1877	426	5220	8704	13 924
	1	82	1960	1037	4577	9745	14 322
	2	88	1843	1782	4041	10 688	14 729

Table 2
Operation cost of predefined and optimized AGC participation factors for Case 1.

Budget	Total operation cost ($)	
	Predefined AGC	Optimized AGC
0	13 924	13 924
1	14 791	14 320
2	15 482	14 728

5.1.1. Impact of uncertainty budgets

Since there are 2 wind farms, the uncertainty budget can vary from 0 to 2. Results are summarized in Table 1. The budget $\sigma = 0$ degenerates into a deterministic optimization problem with no wind power variation. The budget $\sigma = 2$ degenerates into the nonadjustable bounded interval method in the classical LDRs based adjustable robust models [31,32], which is the most conservative situation. We can see that the total operation cost increases steadily with the increasing uncertainty budget. This is because a larger uncertain budget corresponds to the more severe wind power fluctuations, which leads to a more conservative solution. This will result in more units generate more energy or consume more gas uneconomically to deal with the worst-case available wind power scenario. By increasing the uncertainty budget, the solution becomes more robust at the expense of higher operation costs. In our proposed LDRs based adjustable robust model, the robustness level is controlled using a parameter denominated as the budget of uncertainty, leading to significantly less conservative and more practical solutions. It should be noted that the robust solutions here only reveal the operation cost in the worst-case scenario, the actual solutions can be better than the displayed results.

5.1.2. Impact of AGC participation factors

The traditional participation factors of AGC units are generally predefined according to their unit capacity [46], i.e., $\alpha_g = \overline{P}_g^G / \sum_{g=1}^{\mathcal{G}} \overline{P}_g^G$, so the AGC participation factors are fixed. In our LDRs based adjustable robust model, the AGC participation factors are treated as optimization variables, aimed at improving the operational economy. To verify the effect of optimizing the AGC participation factors, the operation cost is compared with the traditional predefined participation factors method [29,30], shown in Table 2. We can see that optimizing AGC participation factors can reduce the operation cost by up to 5.1%. This is because different participation factors correspond to different allocations of wind power among AGC units. If fixed participation factors are adopted, the large-capacity unit has a large participation factor, so its allocated wind power is also large. However, the unit cost for providing the reserve of the large-capacity unit is not necessarily low, which leads to an increase in operation cost.

5.1.3. Convergence performance

The proposed distributed approach is compared with the traditional centralized method. The iteration processes of the natural gas exchanges of NGUs among EO, GO, and CO and the total operation cost are depicted in Figs. 4 and 6, respectively, summarized in Table 1. We can see that the distributed solutions with different uncertainty budgets converge after 33, 82, and 88 iterations. The converged natural gas exchanges of NGUs and the operation cost found

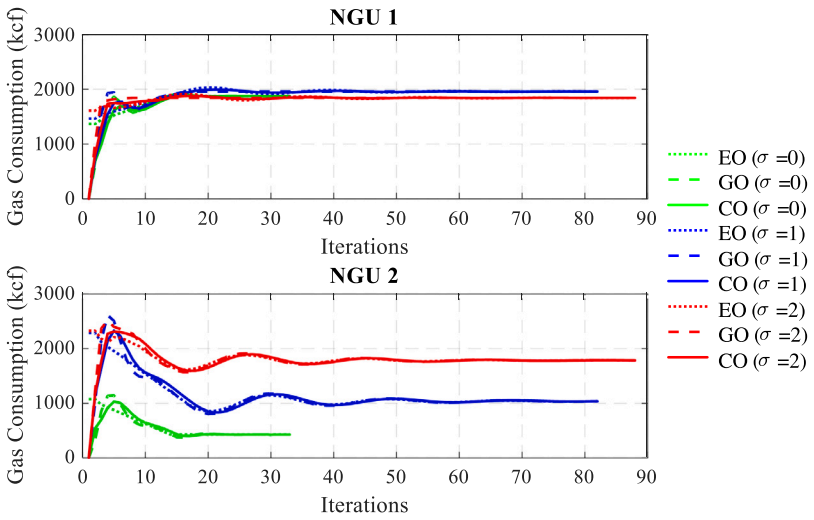

Fig. 4. Convergence curve of natural gas exchange for Case 1 (a) NGU 1 (b) NGU 2.

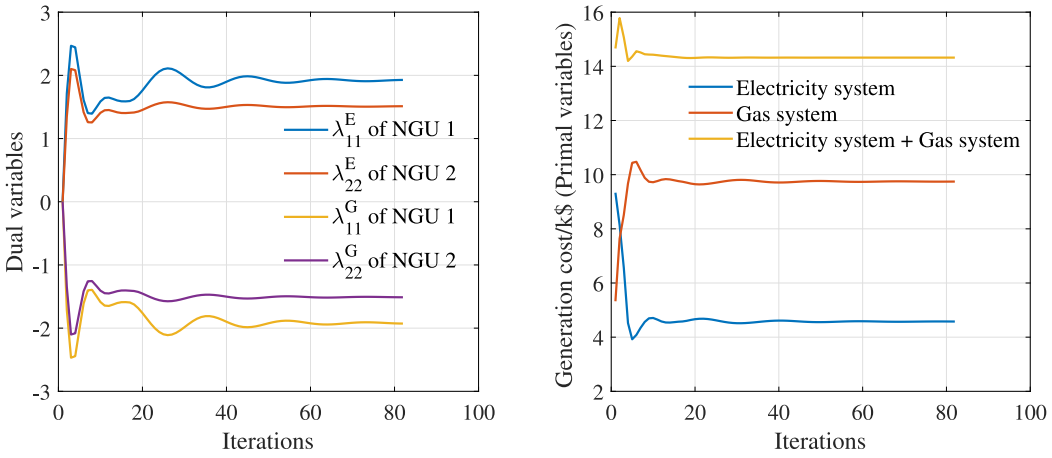

Fig. 5. Convergence curve of dual variables and generation cost for Case 1.

by the distributed method are nearly the same as that identified by the centralized method.

The values of dual variables $(\lambda^{G}_{mi}, \lambda^{E}_{mi})$ for the consensus constraint (18) imply the strength of the coupling between the gas network and the electricity network such that it further indicates how collaborative the gas system and the electricity system are operated. Fig. 5 shows the convergence of dual variables $(\lambda^{E}_{mi}, \lambda^{G}_{mi})$ in constraint (18) and the generation costs (functions of the primal variables) with the budget $\sigma = 1$ as an example. Since ADMM is an augmented Lagrangian based operator splitting approach [43], the generation costs of the electricity network and gas network at the first iteration are equal to the costs of operating the electricity system and gas system independently as the dual variables are initialized by zero. Following the convergence of dual variables, the generation cost is also changed and converges to the optimal.

5.2. 118-Bus-20-Node IEGS

The modified IEEE 118-bus electricity network is assumed interconnected with a 20-node natural gas network [47] in Case 2. The system includes 3 NGUs, 51 non-NGUs, 5 wind farms, 186 branches, 91 electricity loads, 3 natural gas wells, 2 natural gas storages, 19 pipelines, 3 compressors, and 10 gas loads. Convergence tolerance of the primal and dual residues is 0.1 kcf. Variations of wind generation and other algorithm parameters for ADMM are the same as Case 1.

5.2.1. Impact of uncertainty budgets

Case 2 is also optimized with varying budgets and illustrated in Table 3. The total operation cost increases with the increasing uncertainty budgets. This means a larger uncertain budget corresponds to a more conservative solution. Similar to Case 1, when the budget $\sigma = 5$ degenerates into the nonadjustable bounded interval method with the most conservative situation. After the uncertainty budget is greater than the number of wind farms, the robustness level and operation costs do not change, since all uncertain parameters have adopted their worst-case realization values and there is no further uncertain parameter to change.

5.2.2. Impact of AGC participation factors

The traditional predefined participation factors method is also compared with the proposed optimized participation factors model in Case 2, shown in Table 4. We can conclude that the proposed optimized AGC participation factors method can greatly reduce the total operation cost and make the solution less conservative. Additionally, the intention of involving AGC reference output base-points is to account for how the AGC units will respond to the power mismatch caused by wind power uncertainties, but not to generate signals to control the actual output of AGC units. Output base-points are provided to AGC units for reference only, and the actual power outputs of these units are ultimately controlled by the AGC system to compensate the area control error. Noted that this proposed LDRs based adjustable robust OPGF model

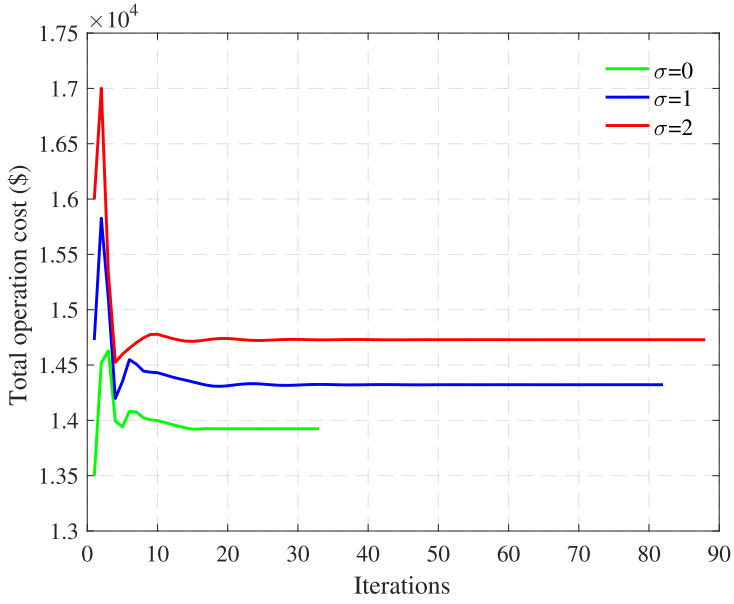

Fig. 6. Convergence curve of total operation cost for Case 1.

Table 3
Comparisons with varying budgets for Case 2.

Scheme	Budget	Iter.	Operation cost ($)			Time (s)
			EO	GO	Total	
Cen.	0	\	53 940	32 205	86 145	6.4
	1	\	54 090	32 201	86 291	7.9
	2	\	54 333	32 145	86 478	9.2
	3	\	54 595	32 090	86 685	9.5
	4	\	54 838	32 060	86 898	8.2
	5	\	54 976	32 045	87 021	11.0
Dis.	0	29	53 940	32 205	86 145	26.7
	1	23	54 089	32 202	86 291	24.4
	2	24	54 333	32 145	86 478	23.7
	3	22	54 596	32 089	86 685	25.5
	4	22	54 838	32 059	86 897	23.1
	5	22	54 977	32 044	87 021	28.7

Table 4
Operation cost of predefined and optimized AGC participation factors for Case 2.

Budget	Total operation cost ($)	
	Optimized AGC	Predefined AGC
0	86 145	86 145
1	86 291	86 702
2	86 478	87 313
3	86 685	88 124
4	86 898	88 570
5	87 021	89 169

can simultaneously optimize the AGC participation factors, utilize the budget of uncertainty in a polyhedral uncertainty set, and consider the wind power curtailment situation, which leads to significantly less conservative and more practical solutions.

5.2.3. Convergence performance

The convergence curve of the total operation cost is depicted in Fig. 7 and summarized in Table 3. We can see that the distributed solutions with different uncertainty budgets nearly coincide with the traditional centralized approach after 29, 23, 24, 22, 22, and 22 iterations, respectively. The solutions from the distributed and the centralized approach are close, which indicates the effectiveness and high solution quality of the distributed approach. The comparison of computation time with the traditionally centralized model is also shown

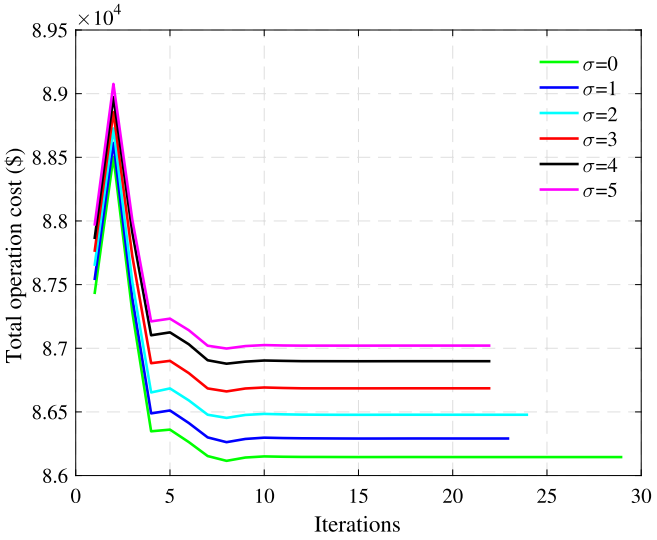

Fig. 7. Convergence curve of total operation cost for Case 2.

in Table 3. The required computation time of the proposed distributed model is slightly higher than the centralized model. Since only a limited set of information is shared among system operators, communication burdens, which usually account for more processing time in practice, are alleviated and information privacy is preserved. With the growth in the IEGS scale, the centralized model will become more difficult to deploy as it requires data for both power system and gas system which generally correspond to different market regulations or administrative jurisdictions. This LDRs based adjustable robust model can also reduce the computation burden of each ADMM iteration and guarantee the convergence of ADMM, which eliminates the need for using any master-subproblem decomposition strategy and can be easily applied to distributed optimization.

The only parameter that affects the convergence performance is the penalty parameter ρ. Theoretically, the choice of ρ does not affect the convergence guarantee. But of course, its value affects the numerical performance. As shown in Table 3, the different budgets have little impact on the iterations and computation time, thus we test the sensitivity

Table 5
Impact of ρ on iterations for Case 2.

ρ	Iterations	Time (s)
0.02	36	44.3
0.002	22	25.5
0.0002	43	60.1

Table 6
Optimality gap for Cases 1 and 2.

Cases	Total operation cost ($)		Optimality gap
	NLP	SOCP	
1	14 392	14 320	0.5%
2	86 721	86 685	0.04%

of the results to ρ with the budget $\sigma = 3$. Results are shown in Table 5. We can see that the iteration numbers of distributed optimization depend on the value of ρ. In order to improve the convergence efficiency of distributed optimization, a careful selection of ρ is essential.

5.3. Accuracy of second-order cone relaxation

We solve the original nonlinear programming (NLP) model by IPOPT as a heuristic method to measure the optimality gap of SOC relaxations, presented in Table 6. The uncertainty budgets in Cases 1 and 2 are respectively $\sigma = 1$ and $\sigma = 3$. We can observe that the optimality gap is relatively small. Besides, these gaps can be mitigated by adjusting gas linepacks. Therefore, the SOC relaxation for the natural gas system is assumed to be exact. In practice, sufficient conditions for an exact SOC relaxation of natural gas flow represent an open issue for further research.

5.4. Discussion

5.4.1. Algorithm 1 vs. Algorithm 2

To compare the communication efficiency of the proposed Algorithm 1 and Algorithm 2, numbers of information units exchanged in the distributed procedure are compared. One information unit is defined as transforming one variable (including the gas consumption of an NGU and consensus variables) from one subsystem to another. In Case 1, the numbers of information units exchanged per iteration in Algorithm 1 and Algorithm 2 are 12 and 8, respectively. While in Case 2, they are 18 and 12, respectively. The numbers of information units exchanged per iteration in Algorithm 2 is one-third smaller than that of Algorithm 1, which indicates that Algorithm 2 is a more communicational efficient method and can help reduce the communication bottleneck. Algorithm 2 is more flexible and robust in response to system changes since no detailed data need to be collected at the central controller.

5.4.2. Applicability and extensibility

The traditional centralized method can be only used for a case in which the natural gas and electricity networks are operated by a vertically integrated utility. Unfortunately, this is an unrealistic assumption, because natural gas and electricity networks are generally managed by different operators in real life. The proposed ADMM based operation structures for two possible infrastructure networks based IEGS (e.g. Great Britain, China, and South American counties [8,9]) have strong applicability where strict claims for reducing communication and privacy preservation burdens are met. The individual operator in power sector and gas sector can operate their respective systems independently, and the information privacy and decision-making independence are preserved among different operators.

In real applications, the regional subproblems of the gas system and the electricity system can be simultaneously implemented by local computers in parallel. Compared to the centralized framework, the proposed distributed method is, thus, potentially more efficient on computation w.r.t the size of the problem that can be addressed and on communication w.r.t the size of information exchanged between the gas and electricity systems. Moreover, only a mild level of accuracy required in practice further improves the effectiveness of the proposed distributed algorithm.

Although the electricity system operator may not have direct control over generating units under the electricity market environment, the generating units can only submit their offering curves to the independent system operator (ISO) according to the market rules. For instance, in the PJM electricity market, generating units cannot determine their own power output. Instead, ISO will clear the market and directly send the cleared quantities to generating units. Thus, the proposed model is practical.

These two Algorithms can be straightforwardly extended to a multi-period operation model considering line-pack. When the discrete decisions (e.g. gas direction) for the long-term operation problem of IEGS are included, some ADMM based heuristic procedure [48] can be adopted to enhance the convergence performance. When the nonlinear constraints (e.g. AC power flow equation) are included, another distributed optimization approach, called Augmented Lagrangian based Alternating Direction Inexact Newton [49], can be adopted to guarantee locally quadratic convergence for AC power flow.

6. Conclusions

This paper considered the operation problem of IEGS and presented the distributed adjustable robust OPGF model. The linear decision rules are improved to reformulate the adjustable robust OPGF model as a computationally tractable problem while simultaneously optimizing the AGC participation factors, utilizing the controllable polyhedral uncertainty set, and considering the wind power curtailment situation. The main conclusions include: (1) The potential of AGC systems in dealing with renewable energy uncertainty is fully exploited, and the budget of uncertainty is used to control the solution robustness level. (2) This improved LDRs based adjustable robust approach can reduce the computational burden caused by the existing decomposition based robust approach when applied to distributed optimization. (3) Based on two possible topological IEGS, i.e., with and without a central coordinator, two tailored ADMM algorithms are proposed to solve subproblems individually in parallel.

CRediT authorship contribution statement

Junyi Zhai: Conceptualization, Software, Investigation, Data curation, Funding acquisition, Writing – original draft. **Yuning Jiang:** Methodology, Validation, Writing – review & editing, Writing – original draft. **Jianing Li:** Formal analysis, Writing – review & editing. **Colin N. Jones:** Supervision, Funding acquisition. **Xiao-Ping Zhang:** Validation, Supervision.

Declaration of competing interest

The authors declare that they have no known competing financial interests or personal relationships that could have appeared to influence the work reported in this paper.

Appendix

Notation: Appendix uses boldface lower case and upper case letters to represent vectors and matrices, respectively.

A.1. Derivation for line flow limit

It is desired to derive the LDRs of (4d) using the full-set formulation that makes use of the sparse network equations directly in the problem. To this end, the power balance under the realization of wind generation can be written in matrix format:

$$\boldsymbol{P}^G + \boldsymbol{P}^W - \boldsymbol{B}\theta = \boldsymbol{P}^D, \tag{29}$$

where $\boldsymbol{P}^G$, $\boldsymbol{P}^W$, $\boldsymbol{P}^D$, and θ denote vectors of the corresponding quantities and $\boldsymbol{B}$ is the network admittance matrix. By taking the first bus as the reference in (4e), the bus angles can be computed as:

$$\theta = \tilde{\boldsymbol{B}}\left(\boldsymbol{P}^G + \boldsymbol{P}^W - \boldsymbol{P}^D\right), \tag{30}$$

where $\tilde{\boldsymbol{B}} = \begin{bmatrix} 0 & \boldsymbol{0}_{1\times(n-1)} \\ \boldsymbol{0}_{(n-1)\times 1} & \dot{\boldsymbol{B}}^{-1} \end{bmatrix}$ and n denote the number of buses in power network, $\dot{\boldsymbol{B}}$ is the sub-matrix obtained from $\boldsymbol{B}$ by removing the first row and column. Also express (8) in vector form:

$$\boldsymbol{P}^W = \hat{\boldsymbol{P}}^W - \beta\xi, \tag{31a}$$

$$\boldsymbol{P}^G = \hat{\boldsymbol{P}}^G - \boldsymbol{\alpha}\left(e^T\xi\right), \tag{31b}$$

where e^T is a vector of ones, $\boldsymbol{\alpha}$ denotes vector of adjustable term associate with unit output, $\boldsymbol{\beta}$ denotes matrix of adjustable term associate with wind generation, ξ denotes vector of wind forecast errors. Substituting (31a) and (31b) in (30) reveals that the bus angles have two components, $\hat{\theta}$ that represents the non-adjustable term corresponding to the wind forecasts and $\Delta\theta$ that represents the adjustable term varying with the uncertain wind forecast error:

$$\theta = \hat{\theta} + \Delta\theta, \tag{32a}$$

$$\hat{\theta} = \tilde{\boldsymbol{B}}\left(\hat{\boldsymbol{P}}^G + \hat{\boldsymbol{P}}^W - \boldsymbol{P}^D\right), \tag{32b}$$

$$\Delta\theta = \tilde{\boldsymbol{B}}\left[-\beta\xi - \boldsymbol{\alpha}\left(e^T\xi\right)\right]. \tag{32c}$$

Note that $\tilde{\boldsymbol{B}}$ is a dense matrix while $\boldsymbol{B}$ is sparse in all practical power networks; because the power network should be balanced at any point in time, (32b) that governs the bus angles $\hat{\theta}$ can be equivalently expressed using the elements of the sparse network admittance matrix:

$$\hat{P}_i^G + \hat{P}_i^W - \sum_{j\in B_i}\frac{\hat{\theta}_i - \hat{\theta}_j}{x_{ij}} = P_i^D,\ \hat{\theta}_1 = 0,\ i \in \mathcal{B}. \tag{33}$$

Expanding (32c) gives

$$\Delta\theta = -\tilde{\boldsymbol{B}}\beta\xi - \tilde{\boldsymbol{B}}\boldsymbol{\alpha}\left(e^T\xi\right). \tag{34}$$

From (34), the change in the angle of bus i due to the uncertain wind forecast error is

$$\Delta\theta_i = -\sum_{k\in\mathcal{W}}\tilde{B}_{ik}\beta_{ik}\xi_k - \left(\sum_{g\in\mathcal{G}}\tilde{B}_{ig}\alpha_g\right)\sum_{k\in\mathcal{W}}\xi_k \tag{35a}$$

$$= -\sum_{k\in\mathcal{W}}\left(\tilde{B}_{ik}\beta_{ik} + \sum_{g\in\mathcal{G}}\tilde{B}_{ig}\alpha_g\right)\xi_k. \tag{35b}$$

Similarly, the change in the angle of bus j is

$$\Delta\theta_j = -\sum_{k\in\mathcal{W}}\left(\tilde{B}_{jk}\beta_{jk} + \sum_{g\in\mathcal{G}}\tilde{B}_{jg}\alpha_g\right)\xi_k. \tag{36}$$

The uncertain power flow in branch ij can be now obtained from (4d), (32a), (35), and (36):

$$\begin{aligned} P_{ij} &= \frac{1}{x_{ij}}\left(\hat{\theta}_i - \hat{\theta}_j + \Delta\theta_i - \Delta\theta_j\right) \\ &= \frac{1}{x_{ij}}\left[\hat{\theta}_i - \hat{\theta}_j + \sum_{k\in\mathcal{W}}\left(\tilde{B}_{jk}\beta_{jk} - \tilde{B}_{ik}\beta_{ik} + \sum_{g\in\mathcal{G}}\tilde{B}_{jg}\alpha_g - \sum_{g\in\mathcal{G}}\tilde{B}_{ig}\alpha_g\right)\xi_k\right]. \end{aligned} \tag{37}$$

A.2. LDRs adjustable robust form

The LDRs based adjustable robust form for the left hand side of (4c) is as follows:

$$\hat{P}_g^G - \underline{P}_g^G \geq \sigma\mu_g^{G(l)} + \sum_{k\in\mathcal{W}} s\left(\kappa_{gk}^{G(l)+} + \kappa_{gk}^{G(l)-} + \kappa_{gk}^{G(l)1}\right) \tag{38a}$$

$$\alpha_g\Delta P_k^W \leq \kappa_{gk}^{G(l)+} + \kappa_{gk}^{G(l)1} + \mu_g^{G(l)} \tag{38b}$$

$$-\alpha_g\Delta P_k^W \leq \kappa_{gk}^{G(l)-} + \kappa_{gk}^{G(l)1} + \mu_g^{G(l)} \tag{38c}$$

$$\kappa_{gk}^{G(l)+} \geq 0,\ \kappa_{gk}^{G(l)-} \geq 0,\ \kappa_{gk}^{G(l)1} \geq 0,\ \mu_g^{G(l)} \geq 0 \tag{38d}$$

$\forall g \in \mathcal{G}, \forall k \in \mathcal{W}$.

The LDRs based adjustable robust form for the left hand side of (4b) is as follows.

$$\hat{P}_j^W \geq \sum_{k\in\mathcal{W}}\left(\kappa_{jk}^{W(l)+} + \kappa_{jk}^{W(l)-} + \kappa_{jk}^{W(l)1}\right) + \sigma\mu_j^{W(l)}, j \in \mathcal{W} \tag{39a}$$

$$\left(\beta_{jk}+1\right)\Delta P_k^W \leq \kappa_{jk}^{W(l)+} + \kappa_{jk}^{W(l)1} + \mu_j^{W(l)},\ j = k \tag{39b}$$

$$-\left(\beta_{jk}+1\right)\Delta P_k^W \leq \kappa_{jk}^{W(l)-} + \kappa_{jk}^{W(l)1} + \mu_j^{W(l)},\ j = k \tag{39c}$$

$$\beta_{jk}\Delta P_k^W \leq \kappa_{jk}^{W(l)+} + \kappa_{jk}^{W(l)1} + \mu_j^{W(l)},\ j \in \mathcal{W}, j \neq k \tag{39d}$$

$$-\beta_{jk}\Delta P_k^W \leq \kappa_{jk}^{W(l)-} + \kappa_{jk}^{W(l)1} + \mu_j^{W(l)},\ j \in \mathcal{W}, j \neq k \tag{39e}$$

$$\kappa_{jk}^{W(l)+} \geq 0,\ \kappa_{jk}^{W(l)-} \geq 0,\ \kappa_{jk}^{W(l)1} \geq 0,\ \mu_j^{W(l)} \geq 0. \tag{39f}$$

The LDRs based adjustable robust form for the left hand side of (4d) is as follows.

$$\overline{L}_{ij} - \frac{\hat{\theta}_i - \hat{\theta}_j}{x_{ij}} \geq \sum_{k\in\mathcal{W}}\left(\kappa_{ijk}^{L(l)+} + \kappa_{ijk}^{L(l)-} + \kappa_{ijk}^{L(l)1}\right) + \sigma\mu_{ij}^{L(l)} \tag{40a}$$

$$-\frac{1}{x_{ij}}\left(\tilde{B}_{jk}\beta_{jk} - \tilde{B}_{ik}\beta_{ik} + \sum_{g\in\mathcal{G}}\tilde{B}_{jg}\alpha_g - \sum_{g\in\mathcal{G}}\tilde{B}_{ig}\alpha_g\right)\Delta P_k^W$$

$$\leq \kappa_{ijk}^{L(l)+} + \kappa_{ijk}^{L(l)1} + \mu_{ij}^{L(l)} \tag{40b}$$

$$\frac{1}{x_{ij}}\left(\tilde{B}_{jk}\beta_{jk} - \tilde{B}_{ik}\beta_{ik} + \sum_{g\in\mathcal{G}}\tilde{B}_{jg}\alpha_g - \sum_{g\in\mathcal{G}}\tilde{B}_{ig}\alpha_g\right)\Delta P_k^W$$

$$\leq \kappa_{ijk}^{L(l)-} + \kappa_{ijk}^{L(l)1} + \mu_{ij}^{L(l)} \tag{40c}$$

$$\kappa_{ijk}^{L(l)+} \geq 0,\ \kappa_{ijk}^{L(l)-} \geq 0,\ \kappa_{ijk}^{L(l)1} \geq 0,\ \mu_{ij}^{L(l)} \geq 0 \tag{40d}$$

$$\forall (i,j) \in \mathcal{L}, \forall k \in \mathcal{W}.$$

References

[1] EIA. Annual energy outlook. 2018.

[2] Zhang X, Shahidehpour M, Alabdulwahab A, Abusorrah A. Security-constrained co-optimization planning of electricity and natural gas transportation infrastructures. IEEE Trans Power Syst 2015;30(6):2984–93.

[3] Correaposada CM, Sanchezmartin P. Security-constrained optimal power and natural-gas flow. IEEE Trans Power Syst 2014;29(4):1780–7.

[4] Wang C, Wei W, Wang J, Liu F, Qiu F, Correaposada CM, Mei S. Robust defense strategy for gas celectric systems against malicious attacks. IEEE Trans Power Syst 2017;32(4):2953–65.

[5] Zhang Y, Le J, Zheng F, Zhang Y, Liu K. Two-stage distributionally robust coordinated scheduling for gas-electricity integrated energy system considering wind power uncertainty and reserve capacity configuration. Renew Energy 2019;135:122–35.

[6] Sánchez CB, Bent R, Backhaus S, Blumsack S, Hijazi H, van Hentenryck P. Convex optimization for joint expansion planning of natural gas and power systems. In: 2016 49th hawaii international conference on system sciences (hicss). 2016, p. 2536–45.

[7] Borrazsanchez C, Bent R, Backhaus S, Hijazi H, Van Hentenryck P. Convex relaxations for gas expansion planning. Informs J Comput 2016;28(4):645–56.
[8] Rudnick H, Barroso LA, Cunha G, Mocarquer S. A natural fit: Electricity-gas integration challenges in south america. IEEE Power Energy Mag 2014;12(6):29–39.
[9] Qadrdan M, Wu J, Jenkins N, Ekanayake J. Operating strategies for a GB integrated gas and electricity network considering the uncertainty in wind power forecasts. IEEE Trans Sustain Energy 2014;5(1):128–38.
[10] Kargarian A, Fu Y, Wu H. Chance-constrained system of systems based operation of power systems. IEEE Trans Power Syst 2016;31(5):3404–13.
[11] Kargarian A, Fu Y, Li Z. Distributed security-constrained unit commitment for large-scale power systems. IEEE Trans Power Syst 2015;30(4):1925–36.
[12] Zhou M, Zhai J, Li G, Ren J. Distributed dispatch approach for bulk ac/dc hybrid systems with high wind power penetration. IEEE Transactions on Power Systems 2018;33(3):3325–36.
[13] Chen Z, Guo C, Dong S, Ding Y, Mao H. Distributed robust dynamic economic dispatch of integrated transmission and distribution systems. IEEE Trans Ind Appl 2021;1.
[14] Zhai J, Jiang Y, Shi Y, Jones CN, Zhang X. Distributionally robust joint chance-constrained dispatch for integrated transmission-distribution systems via distributed optimization. IEEE Trans Smart Grid 2022;accepted.
[15] Jiang Y, Sauerteig P, Houska B, Worthmann K. Distributed optimization using aladin for mpc in smart grids. IEEE Trans Control Syst Technol 2021;29(5):2142–52.
[16] Gao H, Wang J, Liu Y, Wang L, Liu J. An improved admm-based distributed optimal operation model of ac/dc hybrid distribution network considering wind power uncertainties. IEEE Syst J 2020;1–11.
[17] Manshadi SD, Liu G, Khodayar ME, Wang J, Dai R. A distributed convex relaxation approach to solve the power flow problem. IEEE Syst J 2020;14(1):803–12.
[18] Liu C, Wang J, Fu Y, Koritarov V. Multi-area optimal power flow with changeable transmission topology. IET Gener Transm Distrib 2014;8(6):1082–9.
[19] Li Z, Guo Q, Sun H, Wang J. A new lmp-sensitivity-based heterogeneous decomposition for transmission and distribution coordinated economic dispatch. IEEE Trans Smart Grid 2018;9(2):931–41.
[20] Bakirtzis AG, Biskas PN. A decentralized solution to the dc-opf of interconnected power systems. IEEE Trans Power Syst 2003;18(3):1007–13.
[21] Lin C, Wu W, Zhang B, Wang B, Zheng W, Li Z. Decentralized reactive power optimization method for transmission and distribution networks accommodating large-scale dg integration. IEEE Trans Sustain Energy 2017;8(1):363–73.
[22] Wen Y, Qu X, Li W, Liu X, Ye X. Synergistic operation of electricity and natural gas networks via admm. IEEE Trans Smart Grid 2018;9(5):4555–65.
[23] He Y, Yan M, Shahidehpour M, Li Z, Guo C, Wu L, Ding Y. Decentralized optimization of multi-area electricity-natural gas flows based on cone reformulation. IEEE Trans Power Syst 2018;33(4):4531–42.
[24] Wang C, Wei W, Wang J, Bai L, Liang Y, Bi T. Convex optimization based distributed optimal gas-power flow calculation. IEEE Trans Sustain Energy 2018;9(3):1145–56.
[25] Qi F, Shahidehpour M, Li Z, Wen F, Shao C. A chance-constrained decentralized operation of multi-area integrated electricity–natural gas systems with variable wind and solar energy. IEEE Trans Sustain Energy 2020;11(4):2230–40.
[26] He C, Wu L, Liu T, Shahidehpour M. Robust co-optimization scheduling of electricity and natural gas systems via admm. IEEE Trans Sustain Energy 2017;8(2):658–70.
[27] Bertsimas D, Litvinov E, Sun XA, Zhao J, Zheng T. Adaptive robust optimization for the security constrained unit commitment problem. IEEE Trans Power Syst 2013;28(1):52–63.
[28] Zhai J, Zhou M, Li J, Zhang X, Li G, Ni C, Zhang W. Hierarchical and robust scheduling approach for vsc-mtdc meshed ac/dc grid with high share of wind power. IEEE Trans Power Syst 2021;36(1):793–805.
[29] Li Z, Wu W, Zhang B, Wang B. Adjustable robust real-time power dispatch with large-scale wind power integration. IEEE Trans Sustain Energy 2015;6(2):357–68.
[30] Zhao J, Zheng T, Litvinov E. Variable resource dispatch through do-not-exceed limit. IEEE Trans Power Syst 2015;30(2):820–8.
[31] Jabr RA, Karaki S, Korbane JA. Robust multi-period opf with storage and renewables. IEEE Trans Power Syst 2015;30(5):2790–9.
[32] Jabr RA. Adjustable robust opf with renewable energy sources. IEEE Trans Power Syst 2013;28(4):4742–51.
[33] Attarha A, Scott P, Thiébaux S. Affinely adjustable robust admm for residential der coordination in distribution networks. IEEE Trans Smart Grid 2020;11(2):1620–9.
[34] Dehghan S, Amjady N, Conejo AJ. Adaptive robust transmission expansion planning using linear decision rules. IEEE Trans Power Syst 2017;32(5):4024–34.
[35] Jabr RA. Linear decision rules for control of reactive power by distributed photovoltaic generators. IEEE Trans Power Syst 2018;33(2):2165–74.
[36] Keyaerts N. Gas balancing and Line-pack flexibility. 2012.
[37] Li Y, Li Z, Wen F, Shahidehpour M. Privacy-preserving optimal dispatch for an integrated power distribution and natural gas system in networked energy hubs. IEEE Trans Sustain Energy 2019;10(4):2028–38.
[38] Fluxys. Discussion on gas-network operations: personal communication. 2012.
[39] Liu F, Bie Z, Wang X. Day-ahead dispatch of integrated electricity and natural gas system considering reserve scheduling and renewable uncertainties. IEEE Trans Sustain Energy 2019;10(2):646–58.
[40] Qi F, Shahidehpour M, Wen F, Li Z, He Y, Yan M. Decentralized privacy-preserving operation of multi-area integrated electricity and natural gas systems with renewable energy resources. IEEE Trans Sustain Energy 2020;11(3):1785–96.
[41] He Y, Yan M, Shahidehpour M, Li Z, Guo C, Wu L, Ding Y. Decentralized optimization of multi-area electricity-natural gas flows based on cone reformulation. IEEE Trans Power Syst 2018;33(4):4531–42.
[42] Chen S, Wei Z, Sun G, Cheung KW, Wang D. Identifying optimal energy flow solvability in electricity-gas integrated energy systems. IEEE Trans Sustain Energy 2017;8(2):846–54.
[43] Boyd S, Parikh N, Chu E, Peleato B, Eckstein J. Distributed optimization and statistical learning via the alternating direction method of multipliers. Found Trends Mach Learn 2011;3(1):1–122.
[44] He B, Yuan X. On the o(1/n) convergence rate of the douglas–rachford alternating direction method. SIAM J Numer Anal 2012;50(2):700–9.
[45] https://github.com/JunyiZhai1990/IEGS.
[46] Wei W, Liu F, Mei S. Dispatchable region of the variable wind generation. IEEE Trans Power Syst 2015;30(5):2755–65.
[47] Yang L, Xu Y, Sun H, Zhao X. Two-stage convexification-based optimal electricity-gas flow. IEEE Trans Smart Grid 2020;11(2):1465–75.
[48] Takapoui R, Moehle N, Boyd S, Bemporad A. A simple effective heuristic for embedded mixed-integer quadratic programming. Int J Control 2015;93.
[49] Engelmann A, Jiang Y, Mühlpfordt T, Houska B, Faulwasser T. Toward distributed opf using aladin. IEEE Trans Power Syst 2019;34(1):584–94.